

# Cage opening during N<sub>2</sub> binding to the FeMo-cofactor of Nitrogenase

Johannes Schimpl,<sup>1</sup> Helena M. Petrilli,<sup>2</sup> and Peter E. Blöchl<sup>1</sup>

<sup>1</sup>*Institute for Theoretical Physics, Clausthal University of Technology, D-38678 Clausthal-Zellerfeld, Germany*

<sup>2</sup>*Instituto de Física, Universidade de São Paulo,  
Caixa Postal 66318, 05315-970, São Paulo, SP, Brazil*

(Dated: November 8, 2019)

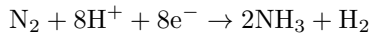
N<sub>2</sub> association to the FeMo-cofactor of nitrogenase, including the recently identified central N ligand, has been investigated using first-principles electronic structure calculations. The oxidation state of the resting state of the cofactor and its electronic structure has been identified. A single proton is added to the sulfur bridges following each electron transfer to the cofactor. During N<sub>2</sub> association, the cofactor undergoes large rearrangements resulting in opening the central Fe-cage of the cofactor. N<sub>2</sub> binds axially while the bond of the bridging SH group breaks. It is then able to insert between the two Fe sites in a bridged configuration.

PACS numbers: 71.15.Nc, 82.20.Kh, 87.15.Rn, 82.39.Rt

Atmospheric nitrogen is the main natural source of nitrogen, which makes up about 10% of the dry mass of biological matter. Before nitrogen molecules can be consumed by organisms, they need to be converted into ammonia, which requires breaking one of the strongest bonds in nature. For this purpose, biological nitrogen fixation employs the enzyme nitrogenase. Nitrogenase consists of two proteins, the Fe protein and the MoFe protein. The latter contains an Fe<sub>7</sub>MoS<sub>9</sub> cluster as the proposed active site. This so-called FeMo-cofactor has been named the most complex bioinorganic cofactor in nature. The crystal structure of nitrogenase was unraveled about ten years ago[1, 2, 3]. Despite intense research, however, the reaction mechanism still remains elusive to date.

A puzzling feature of the FeMo-cofactor was the apparent presence of a cavity surrounded by four iron sites[1, 2, 3]. Most previous ab-initio calculations rested on the assumption that the cage is empty. Recent crystallographic studies[4], however, identified the presence of a central ligand in the cavity, being a C, O, or N atom, which sheds new light on the mechanism of biological nitrogen fixation.

The reaction consumes eight electrons and protons and produces one sacrificial hydrogen molecule[5].



The electron transfer from the Fe protein to the MoFe protein containing the cofactor is the rate limiting factor for nitrogen fixation. Electrons are transferred to the cofactor at a rate of about one to ten per second[6].

A number of reaction mechanisms from nitrogen to ammonia at the FeMo-cofactor have been proposed. They can be classified according to the way N<sub>2</sub> binds to the cofactor: (1) Nitrogen binds head on to one of the six prismatic iron atoms in an ( $\eta_1$ ) coordination[7, 8, 9, 10, 11]. (2) Nitrogen forms a N<sub>2</sub> bridge between two octahedrally coordinated Fe atoms after opening of the cage[12, 13, 14] and (3) N<sub>2</sub> coordinates to Mo[15, 16, 17, 18, 19]. (4) Binding of N<sub>2</sub> to the face formed by four iron sites has

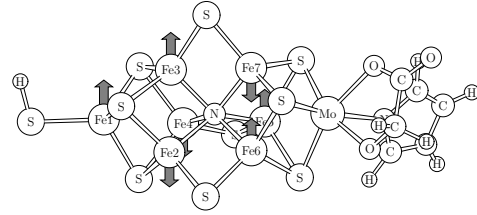


FIG. 1: Resting state of the FeMo-cofactor.

been ruled out with the presence of a central ligand[20].

In this paper we investigate the N<sub>2</sub> binding modes to the FeMo-cofactor using state-of-the-art electronic structure calculations. Inclusion of the central nitrogen ligand dramatically changes our view of the reaction mechanism: The cage of the FeMo cluster opens up upon binding to nitrogen, supporting earlier suggestions that the cluster may undergo major rearrangements during the enzymatic cycle[12]. This indicates that the reaction mechanism is more complex than previously believed. Moreover, we find that N<sub>2</sub> binds to the central cage, whereas binding to the Mo site, a major contender for the role as the reactive site of the cluster, is thermodynamically unstable.

We performed first-principles electronic structure calculations based on density functional theory (DFT)[21, 22] using the PBE functional[23]. We employed the projector-augmented wave method[24] and allowed for a non-collinear description of the spin distribution. The latter is important to properly account for the frustrated antiferromagnetically coupled arrangement of high-spin Fe atoms. The artificial interaction between periodic images of the cluster in our plane-wave based method has been removed[25].

We considered the complete FeMo-cofactor as shown in Fig. 1. The central ligand has been chosen to be nitrogen. The ligands of the FeMo-cofactor have been truncated such that only single bonds were broken, and the open bonds were saturated by hydrogen atoms. Thus we

included an imidazole and a glycolate coordinated to the Mo site to replace the histidine and homocitrate ligands respectively and an SH group instead of a cysteine group at the terminal Fe atom of the cofactor.

The interaction of the cofactor with the surrounding protein has been analyzed using a classical force field, namely the UFF force field[26]. The protein structure, as obtained from the protein data bank entry 1QGU[27], has been included up to a radius of 10 Å and held rigid beyond a radius of 9 Å from FeMoco center and relaxed inside.

Before exploring the N<sub>2</sub> adsorption we need to determine the charge and protonation state of the cofactor. Since the driving forces for protonation and electron transfer are not known a-priori, we derive them by comparing our theoretical with experimental results. This implies identifying the charge state of the resting state and to trace the electron and proton transfer steps until N<sub>2</sub> binds.

A reference is provided by the clear  $S = 3/2$  EPR signal[5] of the resting state. For odd charge states ranging from  $-5e$  to  $+1e$ , we find that only the charge state  $-3e$ , which is collinear, can be clearly identified with an  $S=3/2$  spin state. Charges of  $-1e$  as well as  $+1e$  result in an  $S=1/2$  state, and the charge state of  $-5e$  has a non-collinear spin distribution with  $S = 0.24$ . For the noncollinear clusters we determined the spin state from the absolute value of the integrated spin density. Full structural relaxation in each charge state has been important for the determination of the correct ground state as the spin distribution depends sensitively on the atomic structure.

A charge state  $-3e$  corresponds formally to  $\text{Mo}^{4.5+}\text{Fe}_5^{2.5+}\text{Fe}_2^{2+}\text{N}^{3-}\text{S}_9^{2-}$ , with the ligands contributing a change of  $-3e$ . Six iron atoms form pairs with a parallel spin alignment. The pairs are antiferromagnetically coupled with the neighboring Fe sites as shown in Fig.1. One Fe atom, located next to the Mo site, remains unpaired and is antiferromagnetically coupled to all three of its neighbors. Its spin is oriented in the minority spin direction.

This spin arrangement corresponds to the experimentally observed distribution of four sites aligned with the main spin direction and three antiparallel sites, as found in ENDOR[28, 29] and Mössbauer[30] studies. It should be noted that experiments at higher temperatures may observe an averaged spin structure due to either electronic or structural fluctuations.

The Fe sites are in a distorted tetrahedral environment formed by either four S ligands or three S ligands and the central N-ligand, while the Mo-site is octahedrally coordinated. The bonding network is augmented by metal-metal bonds, derived from the Fe  $e_g$  and Mo  $t_{2g}$  orbitals. While the metal-metal bonds are fairly delocalized, the best formal assignment is to attribute mixed valence bonds to the spin paired Fe atoms and those be-

tween Mo and its three nearest Fe-neighbors. The mixed-valence bonds are limited to the minority spin direction of the participating Fe atoms since the majority spin direction has a filled d-shell. This assignment, derived from an analysis of the off-site elements of the density-of-states, accounts for the total charge and spin for the cluster. In addition it explains the presence of the small magnetic moment of Mo antiparallel to the main spin direction.

Given the good agreement of our calculated atomic structure for the unprotonated cofactor with X-ray[4] and EXAFS[31, 32] experiments, as opposed to the protonated cofactor, we conclude that the resting state is indeed unprotonated.

In order to understand N<sub>2</sub> adsorption, one needs to know the number of protons bound to the cofactor. A reasonable assumption used in our analysis is that the proton transfer rate is fast compared to the slow electron transfer[33, 34, 35, 36]. This implies that the protonation state reaches thermal equilibrium before the next electron is transferred. The protonation state is then determined by the proton chemical potential reflecting the acidity of the cavity containing the cofactor. The proton chemical potential, not accessible in our calculation, will then be calibrated by comparing our findings with experiment.

In order to determine protonation of the cofactor, we investigated the protonation energies of all relevant proton acceptor sites for the singly reduced cofactor. In accordance with previous calculations without central ligand[37], we find that only the bridging sulfur atoms are protonated. Proton addition to the Fe atoms or the  $\mu_3$  sulfur atoms is less favorable by 0.2 eV and 0.5 eV, respectively. A proton added to the Fe-site converts into a hydride ( $\text{H}^-$ ), which can react with a second proton to form a hydrogen molecule.

As obtained from collinear calculations, the proton chemical potential increases by approximately 2.7 eV per proton added to the sulfur bridges and decreases by the same amount for each electron added. This shows that a single proton is added to the cofactor for each additional electron in a ping-pong like manner. Note that the dielectric screening by the environment affects the differences of the calculated protonation energies, but not the qualitative finding of a ping-pong mechanism.

The proton transfer is reflected in a structural change of the cofactor that provides us with a means to relate the protonation state of the cluster to experiment. While electron transfer alone does not change the structure of the cofactor appreciably in our calculations, the protonation decreases the angle of the sulfur bridges, which in turn contracts the cluster. EXAFS measurements indicate that the cluster contracts upon reduction by one electron for *Azotobacter vinelandii*[32], while no significant changes have been found for *Klebsiella pneumoniae*[38]. The fact that proton transfer, as apparent by the contraction, depends on subtle changes of the pro-

tein allows us to identify the proton chemical potential approximately with the first protonation energy of the cofactor reduced by one electron. Knowing the chemical potential we can essentially predict the sequence of electron and proton transfers.

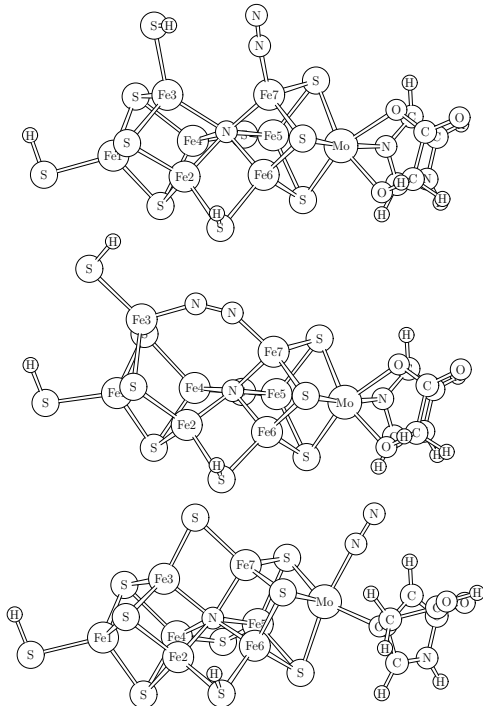


FIG. 2: Structures of the three  $N_2$  binding modes investigated in this work: the open axial mode (top), the bridged mode (middle) and Mo-coordination (bottom).

We have investigated  $N_2$  binding after transfer of one and two electrons with the corresponding number of protons. Our calculations indicate that  $N_2$  binds only in the latter case. Our result that  $N_2$  binds to the doubly protonated cofactor seems to disagree with Thorneley-Lowe scheme[34, 35, 36] which predicts that 3-4 electrons reach the MoFe-protein before  $N_2$  binding. However, EPR measurements during turnover[6] indicate that only two of the three first electrons transferred to the protein actually reach the cofactor. Thus we need to add one electron (and one proton) before comparing our results for the cofactor with the Thorneley-Lowe scheme.

On the basis of the doubly reduced cofactor, we investigated several binding modes of  $N_2$ : On the faces of the central cage, in the bridging position between Mo and Fe, at the Mo site and at the Fe-atoms of the central cage in the axial, equatorial and side-on orientations. All of these complexes have been previously discussed and investigated theoretically for the complex without the central nitrogen ligand. According to our calculation only the adsorption to an Fe atom on the central cage is stable.

Upon adsorption of  $N_2$  to an Fe-site next to a protonated sulfur bridge, we find that the sulfur bridge breaks so that the cage structure of the cofactor is disrupted.

Adsorption and cage opening occur in a concerted mechanism. The resulting structure is shown in Fig 2. The barrier for  $N_2$  adsorption is 0.29 eV, which can be overcome easily by thermal fluctuations. The binding energy is 0.27 eV.

For the cofactor without central ligand, Rod et al.[9] found that  $N_2$  binds in an axial mode to the same Fe-site, but the cage structure of the cofactor remained intact in these calculations. We find that this result changes radically when the central nitrogen ligand is included. Compared to the metastable structure analogous to that of Rod et al., the cage opening stabilizes  $N_2$  binding by 0.55 eV, indicating that  $N_2$  does not bind unless the sulfur bridge breaks away. The structure with a closed cage is metastable, with a small barrier of only 0.1 eV towards the ground state.

With an N-H distance of 2.8 Å, the SH group seems to be well positioned for the first protonation of dinitrogen, which is believed to have the largest energy barrier in the catalytic cycle. However, according to our calculations, this proton transfer is energetically not favorable.

The axial binding mode is not the only possible configuration for the  $N_2$  complex with the FeMo-cofactor. We find that dinitrogen can tilt to form a dinitrogen bridge between the two Fe atoms formerly bridged by a SH group. As dinitrogen binds to the second Fe atom, the bond of this Fe atom to the central ligand breaks, so that the tetrahedral coordination of the Fe atom is retained. This bridging configuration shown in Fig. 2 is energetically more stable by 0.08 eV than the open axial mode. The reaction barrier of 0.68 eV corresponds to a reaction rate somewhat smaller than the electron transfer rate from the Fe protein to the MoFe protein. Thus both structures, with an axial and bridged dinitrogen are equally likely intermediates for the  $N_2$  fixation cycle.

A similar adsorption mode with  $N_2$  bridging two Fe sites has been proposed earlier by Sellmann et al.[13] Sellmann's model differs from our bridged complex in that the Fe sites are octahedrally coordinated, instead of the tetrahedral coordination in our cluster. The different coordination reflects in a major change of the electronic structure: The octahedral complex results in low-spin Fe atoms while the tetrahedral coordination results in high-spin Fe-atoms, which have different chemical behavior. The chemical analogy to octahedral low-spin complexes[39] has been one of the main reasons for Sellmann's proposal.

The additional ligands in Sellmann's model are water molecules and the nitrogen atoms from two amino acids of the protein, glutamine Gln191 and histidine His195[40]. We have investigated the model proposed by Sellmann by modeling the nitrogen ligands with ammonia molecules. We find this structure at least metastable in the absence of the central nitrogen ligand. Addition of the central ligand, however, results in the spontaneous desorption of the three water ligands from

the two bridged Fe sites. The ammonia ligands remain bound to the Fe sites, so that the latter assume a penta-coordinate coordination with high-spin iron atoms.

An important question is if the protein environment is able to accommodate the expansion of the cage after N<sub>2</sub> binding. Therefore we embedded the rigid FeMo-cofactor as obtained from our calculations into the protein simulated with classical force fields.

The cofactor with N<sub>2</sub> adsorbed at sites Fe3 and Fe7 can easily be accommodated both in the open-cage and in the bridged configuration. There is also sufficient space to accommodate N<sub>2</sub> bound to Fe6, even though the embedding energy is 1 eV higher than that for N<sub>2</sub> bound to Fe3 or Fe7. The presence of a nearby imidazole ring of the protein (His $\alpha$ 195)[40] prevents the transition to the bridged configuration as well as adsorption to site Fe2. Binding at sites Fe4 and Fe5 can be excluded, because either the dinitrogen or the SH group collides with the protein backbone in close proximity of site Fe4.

We conclude that the adsorption complexes can be accommodated in the central cage. The most likely adsorption sites are Fe3 and Fe7. Given the uncertainties of the force field calculations we do not explicitly exclude adsorption to Fe6.

Coordination of N<sub>2</sub> to Mo has been discussed in great detail in the literature[15, 16, 17, 18, 19]. While the molybdenum atom in the cofactor stands out, it is not essential. There are other nitrogenases, where the Mo atom of the cofactor is replaced by V or Fe. While their efficiency is reduced their mere existence indicates that the Mo-site is not essential.

The Mo atom is octahedrally coordinated to three sulfur sites of the cofactor, to two oxygen atoms of homocitrate and to the nitrogen atom of a histidine. N<sub>2</sub> association on the Mo atom is initiated by a proton transfer to the carboxyl group of homocitrate. After protonation, the Mo-O bond becomes very labile. Nevertheless, N<sub>2</sub> binding to the vacant coordination site at Mo is unstable by 0.31-0.34 eV irrespective of the protonation state of the carboxyl group of homocitrate. While hydrophobic forces of the environment, not considered in this work, may increase the affinity to N<sub>2</sub>, the presence of more stable binding modes at the Fe sites provides strong evidence that the mechanism does not proceed at the Mo site.

Our finding that binding of N<sub>2</sub> at the Mo site is unfavorable differs from previous conclusions[17, 18] derived from smaller model systems. This difference has been traced to the small cluster size, that is 1-2 metal sites, used in those calculations.

In this work, we analyzed the N<sub>2</sub> adsorption at the FeMo-cofactor of nitrogenase containing the recently detected central nitrogen ligand. Special attention has been given to oxidation states and the sequence of electron and proton transfer steps. We find that N<sub>2</sub> binding results in a disruption of the cage structure of the FeMo-cofactor. In contrast to the obvious assumption that the central

ligand adds rigidity to the cofactor, the additional nitrogen atom offers a variable number of bonds to its Fe neighbors and thus adds flexibility to the structure.

We acknowledge support by the HLRN for granting access to their IBM pSeries 690 Supercomputers.

- 
- [1] J. Kim and D. Rees, *Nature* **360**, 553 (1992).
  - [2] J. Kim and D. Rees, *Science* **257**, 1667 (1992).
  - [3] M. Georgiadis, H. Komiya, P. Chakrabarti, D. Woo, J. Kornuc, and D. Rees, *Science* **257**, 1653 (1992).
  - [4] O. Einsle, F. Tezcan, S. Andrade, B. Schmid, M. Yoshida, J. Howard, and D. Rees, *Science* **297**, 1696 (2002).
  - [5] B. Burges and D. Lowe, *Chem. Rev.* **96**, 2983 (1996).
  - [6] K. Fisher, W. Newton, and D. Lowe, *Biochemistry* **40**, 3333 (2001).
  - [7] I. Dance, *Chem. Commun.* p. 165 (1997).
  - [8] I. Dance, *Chem. Commun.* p. 523 (1998).
  - [9] T. Rod, B. Hammer, and J. Nørskov, *Phys. Rev. Lett.* **82**, 4054 (1999).
  - [10] T. Rod and J. Nørskov, *J. Am. Chem. Soc.* **122**, 12751 (2000).
  - [11] T. Rod, A. Logadottir, and J. Nørskov, *J. Chem. Phys.* **112**, 5343 (2000).
  - [12] R. Thorneley, D. Lowe, I. Dance, D. Sellmann, J. Sutter, D. Coucouvanis, and C. Pickett, *JBIC* **1**, 575 (1996).
  - [13] D. Sellmann, J. Utz, N. Blum, and F. Heinemann, *Coord. Chem. Rev.* **190-192**, 607 (1999).
  - [14] D. Sellmann, A. Fürsattel, and J. Sutter, *Coord. Chem. Rev.* **200-202**, 545 (2000).
  - [15] C. Pickett, *J. Biol. Chem.* **1**, 601 (1996).
  - [16] K. Grönberg, C. Gormal, M. Durrant, B. Smith, and R. Henderson, *J. Am. Chem. Soc.* **120**, 10613 (1998).
  - [17] R. Szilagyi, D. Musaev, and K. Morokuma, *Inorg. Chem.* **40**, 766 (2001).
  - [18] M. Durrant, *Biochemistry* **41**, 13934 (2002).
  - [19] M. Durrant, *Biochemistry* **41**, 13946 (2002).
  - [20] I. Dance, *Chem. Commun.* **3**, 324 (2003).
  - [21] P. Hohenberg and W. Kohn, *Phys. Rev. B* **136**, 864 (1964).
  - [22] W. Kohn and L. Sham, *Phys. Rev. A* **140**, 1133 (1965).
  - [23] J. Perdew, K. Burke, and M. Ernzerhof, *Phys. Rev. Lett.* **77**, 3865 (1996).
  - [24] P. Blöchl, *Phys. Rev. B* **50**, 17953 (1994).
  - [25] P. Blöchl, *J. Chem. Phys.* **103**, 7422 (1986).
  - [26] A. Rappé, C. Casewit, K. Colwell, W. Goddard, and W. Skiff, *J. Am. Chem. Soc.* **114**, 10024 (1992).
  - [27] S. Mayer, D. Lawson, C. Gormal, S. Roe, and B. Smith, *J. Mol. Biol.* **292**, 871 (1999).
  - [28] R. Venter, M. Nelson, P. McLean, A. True, M. Levy, B. Hoffman, and W. Orme-Johnson, *J. Am. Chem. Soc.* **108**, 3487 (1986).
  - [29] A. True, M. Nelson, R. Venter, W. Orme-Johnson, and B. Hoffman, *J. Am. Chem. Soc.* **110**, 1935 (1988).
  - [30] S. Yoo, H. Angove, V. Papaefthymiou, B. Burgess, and E. Münck, *J. Am. Chem. Soc.* **122**, 4926 (2000).
  - [31] I. Harvey, R. Strange, R. Schneider, C. Gormal, C. Garner, S. Hasnain, R. Richards, and B. Smith, *Inorg. Chim. Acta* **275-276**, 150 (1998).
  - [32] J. Christiansen, R. Tittsworth, B. Hales, and S. Cramer, *J. Am. Chem. Soc.* **117**, 10017 (1995).

- [33] F. Simpson and R. Burris, *Science* **224**, 1095 (1984).
- [34] R. Thorneley and D. Lowe, *Biochem. J.* **224**, 887 (1984).
- [35] D. Lowe and R. Thorneley, *Biochem. J.* **224**, 895 (1984).
- [36] R. Thorneley and D. Lowe, *Biochem. J.* **224**, 903 (1984).
- [37] T. Lovell, J. Li, D. Case, and L. Noodleman, *J. Biol. Inorg. Chem.* **7**, 735 (2002).
- [38] R. Eady, B. Smith, Z. Abraham, F. Dodd, J. Grossmann, L. Murphy, R. Strange, and S. Hasnain, *Journal de physique* **C2**, 611 (1997).
- [39] D. Sellmann and J. Sutter, *J. Biol. Inorg. Chem.* **1**, 597 (1996).
- [40] Our notation refers to nitrogenase of *Azotobacter vinelandii*.